Published in final edited form as:
Cancer Res. 2013 May 1; 73(9): 2782–2794. doi:10.1158/0008-5472.CAN-12-3981.

CSF1R signaling blockade stanches tumor-infiltrating myeloid cells and improves the efficacy of radiotherapy

Jingying Xu[1,2], **Jemima Escamilla**[1,2], **Stephen Mok**[1], **John David**[1], **Saul Priceman**[3], **Brian West**[4], **Gideon Bollag**[4], **William McBride**[5], and **Lily Wu**[1,2,6,7]

[1]Department of Molecular and Medical Pharmacology, David Geffen School of Medicine, University of California Los Angeles, Los Angeles, CA 90095, U.S.A.

[2]Institute of Molecular Medicine, David Geffen School of Medicine, University of California Los Angeles, Los Angeles, CA 90095, U.S.A.

[3]Department of Cancer Immunotherapeutics and Tumor Immunology, Beckman Research Institute and City of Hope Comprehensive Cancer Center, Duarte, CA 91010, U.S.A.

[4]Plexxikon Inc., Berkeley, California 94710, U.S.A.

[5]Department of Radiation Oncology, David Geffen School of Medicine, University of California Los Angeles, Los Angeles, CA 90095, U.S.A.

[6]Department of Urology, David Geffen School of Medicine, University of California Los Angeles, Los Angeles, CA 90095, U.S.A.

[7]Department of Pediatrics, David Geffen School of Medicine, University of California Los Angeles, Los Angeles, CA 90095, U.S.A.

Abstract

Radiotherapy is used to treat many types of cancer, but many treated patients relapse with local tumor recurrence. Tumor-infiltrating myeloid cells (TIMs), including CD11b (ITGAM)$^+$F4/80 (EMR1)$^+$ tumor-associated macrophages (TAMs) and CD11b$^+$Gr-1 (LY6G)$^+$ myeloid-derived suppressor cells (MDSCs), respond to cancer-related stresses and play critical roles in promoting tumor angiogenesis, tissue remodeling and immunosuppression. In this report, we employed a prostate cancer model to investigate the effects of irradiation on TAMs and MDSCs in tumor-bearing animals. Unexpectedly, when primary tumor sites were irradiated we observed a systemic increase of MDSCs in spleen, lung, lymph nodes and peripheral blood. Cytokine analysis showed that the macrophage colony-stimulating factor CSF1 increased by 2-fold in irradiated tumors. Enhanced macrophage migration induced by conditioned media from irradiated tumor cells was completely blocked by a selective inhibitor of CSF1R. These findings were confirmed in prostate cancer patients, where serum levels of CSF1 increased after radiotherapy. Mechanistic investigations revealed the recruitment of the DNA damage-induced kinase ABL1 into cell nuclei where it bound the CSF1 gene promoter and enhanced CSF1 gene transcription. When added to radiotherapy, a selective inhibitor of CSF1R suppressed tumor growth more effectively than

Corresponding Author: Lily Wu, M.D. Ph.D., Departments of Molecular & Medical Pharmacology, Urology, 33-118 CHS, UCLA School of Medicine, Los Angeles, CA 90095-1735, Tel: 310-794-4390, lwu@mednet.ucla.edu.

radiation alone. Our results highlight the importance of CSF1/CSF1R signaling in the recruitment of TIMs which can limit the efficacy of radiotherapy. Further, they suggest that CSF1 inhibitors should be evaluated in clinical trials in combination with radiotherapy as a strategy to improve outcomes.

Keywords

radiotherapy; myeloid cells; TAM; MDSC; CSF1; CSF1R; ABL1

Introduction

Radiotherapy (RT) is one of the primary treatments for prostate cancer. Approximately 50% of patients are treated with radiotherapy either alone or in combination with other therapies (1). Data from Cancer of the Prostate Strategic Urologic Research Endeavor (CaPSURE) identified that 63% of patients experienced biochemical PSA recurrence after RT (2). In fact, D'Amico et al determined that a high rate of PSA velocity pretreatment is significantly associated with a shorter time to not only PSA recurrence but also prostate cancer-specific mortality after RT (3), and most of the recurrence is local (4). Several studies have addressed the importance of hypoxia and the SDF-1/CXCR4 axis in promoting tumor regrowth after RT in brain tumor and breast cancer (5, 6). However, a better understanding of the mechanisms of tumor regrowth is needed to achieve increased local control by RT in prostate cancer and improve the cure rate of this disease.

Solid tumors contain a significant population of tumor-infiltrating myeloid cells (TIMs) (7). TIMs are now recognized as important mediators of not only tumor progression and metastasis (8), but also therapeutic resistance (9, 10), through promoting angiogenesis and suppressing antitumor immune responses (11, 12). The pro-tumorigenic role of “alternatively” activated macrophages has been well-established (12). Recently, another specific subtype of TIMs, namely myeloid-derived suppressor cells (MDSCs), is receiving great attention in cancer research. MDSCs comprise a heterogeneous population of immature myeloid cells that originate in the bone marrow and are recruited to the tumor by a diverse array of cytokine and chemokine signals. Similar to tumor-associated macrophages (TAMs) (8), MDSCs have been shown to generate an environment favorable for tumors by heightening immunosuppression, angiogenesis and invasion (13–15). Various cell surface markers are used to identify TIM subsets: TAMs can be identified by CD11b and F4/80, and MDSCs by CD11b and Gr-1 co-expression in murine models (11, 16). Macrophage colony-stimulating factor (M-CSF or CSF1) is a potent growth factor that promotes the differentiation, proliferation, and migration of monocytes/macrophages via signaling through its receptor tyrosine kinase CSF1R (cFMS) (17, 18). We recently showed that TAMs and MDSCs form a spectrum of bone marrow-derived myeloid cells dependent on CSF1/CSF1R signaling for recruitment into the tumor and that they play critical roles in tumor growth (15). DeNardo *et al*. also highlighted the importance of CSF1/CSF1R signaling in the recruitment of TAMs in breast cancer and further showed that CSF1R blockade can inhibit TAMs in chemotherapy and improve treatment outcome (19).

ABL1 (c-Abl) is a ubiquitously expressed non-receptor tyrosine kinase that has been implicated in many cellular processes including cell migration, differentiation, apoptosis and gene regulation (20–22). ABL1 has also been implicated in the proliferation and metastasis of melanoma and breast cancer cells (23–25). In the present study, we show that the infiltration of TIMs is significantly enhanced by local irradiation of prostate cancer. In addition, CSF1 mRNA and CSF1 secretion is increased following radiotherapy through an ABL1-dependent mechanism. We further demonstrated that blockade of CSF1/CSF1R signaling effectively reduces TIMs infiltration to tumors, thereby achieving more effective tumor growth suppression after irradiation. The rational combination therapy reported here may provide a more effective and durable treatment strategy for prostate cancer patients.

Materials and Methods

Cell culture

Murine macrophage RAW264.7 cells (ATCC), ras+myc-transformed RM-1 and RM-9 prostate tumor cells (kind gifts from Dr. Timothy C. Thompson, Baylor College of Medicine), human glioblastoma cell lines U87 and U251 (a kind gift from Dr. Paul Mischel), human breast cancer cell line MDA-MB-283, and mouse malignant peripheral nerve sheath tumor cells (MMPNST, a kind gift from Dr. Hong Wu) were cultured in Dulbecco modified eagle medium (DMEM) containing 10% fetal bovine serum (FBS), 100 U/mL penicillin, and 15mM HEPES at 37°C with 5% CO2. Human prostate cancer cell line CWR and LNCaP, and the human carcinoma cell line A549 were cultured in RPMI-1640 medium containing 10% fetal bovine serum (FBS), 100 U/mL penicillin, and 15mM HEPES at 37°C with 5% CO2. Cell lines were periodically authenticated by morphologic inspection and tested negative for mycoplasm contamination by PCR tests.

Chromatin Precipitation (ChIP)

Treated Myc-CaP cells were cross-linked with 1% formaldehyde at room temperature for 15 minutes. The cells were then washed with PBS and processed by the manufacture's instruction using Pierce® Agarose ChIP Kit (Thermo Scientific). c-Abl antibody K-12 (Santa Cruz) and RNA polymerase II (Santa Cruz) were used for immunoprecipitation. The following primers were used for detecting CSF1 promoter sequences: Forward: 5'ATGTGTCA GTGCCTGTGAGTGTGT3', Reverse: 5'GCCAGGGTGATTTCCCATAAACCA 3'; CSF1 control sequences: Forward, 5'TGCAAGAAGCACCCATGAAATGGC3', Reverse: 5'ATGCCAAAGCCTGCAGTTAAACCC3'.

Human Serum Assessment

Sera from human prostate cancer patients before and after radiotherapy was obtained from by the Department of Radiation Oncology, UCLA Medical Center Hospital, with informed consent according to US federal law and are exempt from consideration by the UCLA Administrative Panel on Human Subjects in Medical Research. Analysis of CSF1 was done by Eve Technologies using human CSF1 multiplex kit (Biorad).

In vivo tumor models

C57BL6 male mice (4–8 weeks old) were purchased from Jackson Laboratory (Bar Harbor). RM-1 (2.5×10^5 cells), RM-9 (2.5×10^5 cells) or Myc-CaP (2×10^6 cells) were implanted subcutaneously in the thigh, and treatment was initiated when tumors reached 4 mm in diameter. All animal experiments were approved by the UCLA IACUC and conformed to all local and national animal care guidelines and regulations.. Tumor size was measured by digital calipers daily or every two days depending on the model. Mice were sacrificed and tissues were analyzed at the ethical tumor size limit of 1.5 cm in diameter. For GW2580 treatment, mice were treated with control diluent (0.5% hydroxypropyl methylcellulose, Sigma-Aldrich; 0.1% Tween20 in distilled H_2O) or GW2580 (160 mg/kg) by oral gavage beginning on the same day irradiation treatment started. PLX3397 was provided in food chow together with daily food consumption.

In vitro migration assay

RAW264.7 (1.5×10^5 cells) were seeded in cell culture inserts (8 μm pore size; BD Falcon) in DMEM containing 0.1% FBS with or without 1000nM GW2580. Inserts were placed in 24-well plates with tumor-conditioned media collected 48hrs after irradiation treatment (3Gy). After 6 hours, migrated cells were immediately fixed in 3% formaldehyde and stained with 4,6-diamidino-2-phenylindole (DAPI). Nine fields/well at 4× magnification were quantified using ImageJ Version 1.34s (National Institute of Health).

Immunohistochemistry

Tissues were harvested and fixed in 3% paraformaldehyde overnight. Sections (5 μm) were stained with the following antibodies: anti-F4/80 (1:500; Serotec), anti-Gr-1 (1:100; eBioscience), or anti-CD31 (1:300; BD Biosciences) antibodies. Histology was performed, processed, and quantified as previously described (15). The samples were analyzed using an Olympus BX41 fluorescent microscope fitted with a Q-Imaging QICAM FAST 1394 camera. Images were captured at 4×, 10×,or 20× magnification using QCapture Pro Version 5.1 (Media Cybernetics), and quantified using ImageJ Version 1.34s (NIH).

Immunofluorescence microscopy

Cells seeded on cover slips were fixed with 3% formaldehyde and incubated with c-Abl antibody (K-12, 1:100, Santa Cruz) followed by AlexaFluor 488 rabbit anti-mouse (Invitrogen) and then AlexaFluor 568 phalloidin and DAPI (Invitrogen). Mounting medium (Pro-Long Gold Antifade Reagent; Invitrogen) was applied and coverslips were sealed with clear nail polish. Fluorescent images were acquired at room temperature on a confocal microscope, LSM710 (Carl Zeiss).

Flow cytometry analysis

To prepare single-cell suspensions for flow cytometry, harvested tissues (tumors, lungs) were dissected into approximately 1- to 3-mm^3 fragments and digested with 80 U/mL collagenase (Invitrogen) in DMEM containing 10% FBS for 1.5 hours at 37°C while shaking. Spleens and lymph nodes were gently dissociated between 2 glass slides for single-cell isolation. Peripheral blood was isolated directly into BD Vacutainer K2 EDTA tubes

(BD Biosciences). After red blood cell (RBC) lysis (Sigma-Aldrich), single-cell suspensions were filtered and incubated for 30 minutes on ice with the following: APC, PerCP-Cy5.5, PE, APC-e780-conjugated antibodies (CD11b, Gr-1, CSF1R and F4/80) were purchased from eBioscience (1:200). Ly6C (1:200) was purchased from BD Bioscience. DAPI was purchased from Invitrogen. Cells were washed twice before analysis on the BD LSR-II flow cytometer (Beckman Coulter). Data was analyzed with FlowJo software (TreeStar).

Local irradiation

Irradiation was performed using a Gulmay X-ray machine (300kV, 10mA) with a dose rate of 1.84 Gy/min. When tumors reach 4–5 mm in diameter, mice were anesthetized and irradiated with a daily dose of 3Gy for 5 days to the tumor area with the rest of body shielded.

Real-time RT-PCR analysis

Total cellular RNA was extracted from cells using Tri Reagent (Sigma Aldrich). RNA was isolated according to the TRIzol procedure. RNA was quantified and assessed for purity by UV spectrophotometry and gel electrophoresis. RNA (1 μg) was reverse-transcribed using iScript cDNA synthesis kit (Biorad) according to manufacturer's instructions. For each sample, 1 μl cDNA (~ 20 ng) was amplified using Syber green 2× master mix (Bioline) and 10 μM primers (Primer sequences are listed in supplemental Table 1). The reaction was run on My IQ single color iCycler real time PCR machine (Biorad). Samples were amplified using the following cycling conditions: 40 cycles of 95°C/15 sec, 60°C/30 sec and 72°C/30 sec. Gene expression was determined by delta Ct method and normalized to β-actin expression.

SDS-PAGE

For experiments using concentrated media, cells were plated in 150mm tissue culture dish in 0% FBS DMEM overnight. 20ml of media was collected 48hrs after irradiation and subjected to media concentration using a protein concentrator (Pierce Biotechnology) at the speed of 4500 g for 30 min. Total volume was normalized between samples and 40 μl was loaded onto 4–12% continuous gradient Tris-glycine gel (Invitrogen). For ABL1 cleavage experiments, cells were plated in 6-well plates overnight and collected after irradiation at the time indicated. Cells were lysed in RIPA buffer (Upstate) containing proteinase inhibitor cocktail (Sigma), sonicated briefly, and centrifuged 10 min at 12,000g. 20 μg of cell lysates was resolved on a 4–12% continuous gradient Tris–glycine gel (Invitrogen). The gels were then transferred to PVDF membrane (Millipore) and incubated with primary antibodies: anti-ABL1 (K-12, rabbit polyclonal, Santa Cruz), dilution 1:1000; anti-CSF1 (H-300, rabbit polyclonal, dilution (1:20,000) Santa Cruz), dilution 1:1000; anti-GAPDH (A-3, mouse monoclonal, Santa Cruz).

Statistical Analysis

Data are presented as mean plus or minus SEM. Statistical comparisons between groups were performed using the Student *t* test.

Results

Local irradiation enhances myeloid cell infiltration to tumors

Abundant evidence points to the infiltrating myeloid cells exerting significant influences on tumor cell aggression and the immunological environment. Hence, we studied irradiation-induced TIMs recruitment in two immunocompetent murine prostate cancer models, namely RM-1 and Myc-CaP syngeneic in the C57/BL6 and FVB strain, respectively. These models provide distinct host genetic background, tumor growth rate, degree of myeloid cells infiltration and response to irradiation to broaden the perspectives on this issue. We first examined the recruitment of TIMs to tumors after irradiation in the RM-1, a Ras- and Myc-transformed murine prostatic cancer model (26), with moderate level of TIMs infiltration. As shown in Figure 1, irradiation effectively delayed the tumor growth by approximately 7 days (Fig 1A). Control tumors and irradiated tumors were collected when they reached similar sizes (day 13 for control tumors and day 19 for irradiated tumors) and processed to assess their content of TIMs. Irradiation significantly induced the infiltration of $F4/80^{+}CD11b^{+}$ TAMs (Fig 1B) and $Gr\text{-}1^{+}CD11b^{+}$ MDSCs (Fig 1C) to the tumors. Immunohistochemistry staining further confirmed this increase of TIMs in the tumors (Fig 1D). Recent reports further distinguished the myeloid subsets within MDSCs as consisting of MO-MDSC ($CD11b^{hi}ly6C^{lo}$) and PMN-MDSC ($CD11b^{lo}ly6C^{hi}$) with different functional characteristics (27). We found that both MO-MDSCs and PMN-MDSCs were significantly induced by irradiation, with MO-MDSCs showing a larger increase (Fig 1E). Likewise, the irradiation-induced TIMs recruitment was also observed in RM-9 tumor, a C57BL6 compatible model derived in the same manner as RM-1, and Myc-CaP tumor, a myc oncogene-driven model implantable in FVB host (Supplemental Fig 1–2). Taken together, these data demonstrated that local irradiation enhances recruitment of both TAMs and MDSCs to tumors in several murine prostate cancer models.

Local irradiation enhances systemic myeloid cell expansion

To better characterize the potential systemic impact of local tumor irradiation, we examined the infiltration of MDSCs and TAMs in peripheral tissues at different time points after irradiation, providing insights on the dynamics and kinetics of the myeloid cell recruitment process. The level of $CD11b^{+}F4/80^{+}$ macrophages were low in lungs, spleens, lymph nodes, and blood, thus we focused on $CD11b^{+}Gr\text{-}1^{+}$ MDSCs in the systemic sites and analyzed the content of $CD11b^{+}F4/80^{+}$ macrophages only in the tumor (Fig 2B). As shown in Figure 2, prior to irradiation, the baseline levels of MDSCs in tumors, blood and spleens were 1.5 ± 0.9%, 30.1 ± 1.3%, and 3.4 ± 1.1%, respectively and the levels in the lungs and lymph nodes were negligible. In untreated mice, MDSC levels stay the same or only mildly increases over time (Fig 2). In irradiated mice, within two days after irradiation, MDSCs in the peripheral blood doubled to 69.0 ± 6.8% (Fig 2C), while MDSCs stayed relatively stable in spleens, lymph nodes and lungs (Fig 2D–2F). In the irradiated tumor, there was a sustained low level of tumoral MDSCs throughout and beyond the duration of irradiation while they increased nearly 4 fold (1.5 ± 0.9% to 6.5 ± 1.9%) in non-irradiated tumors. On day 12, 2 days after cessation of tumor irradiation, MDSC levels reached their nadir in the tumors, but had begun to rise in the other organs. By day 15, a dramatic increase in the MDSC population was observed in the tumor, spleen, and lymph node, with levels reaching a peak of ~15% in all 3

sites (Fig 2A, D, F) before falling on day 17. In the blood and lung the trend of MDSC elevation continued from day 15 on, reaching a remarkable level of 80.0 ± 5.3% and 30.7 ± 14.6%, respectively, on day 17. Collectively, these data suggest that local tumor irradiation induces the expansion of MDSCs and their subsequent influx into different organs in a time-dependent manner.

Irradiation induces macrophage migration and expression of protumorigenic genes

We next used an *in vitro* culture system to aid in dissecting the complex cross-signaling between different cellular components in the tumor microenvironment after irradiation. We first examined the effects of conditioned media from irradiated tumor cells on the migration ability of macrophages. RAW264.7 murine macrophages were analyzed in a transwell migration assay with conditioned media from irradiated or non-irradiated murine prostate cancer cells (RM-1 and Myc-CaP) as the migration stimulus. Conditioned media from irradiated tumor cells induced a nearly two-fold greater number of RAW264.7 cells to migrate across the transwell filter compared to non-irradiated controls (Fig 3A and data not shown for Myc-CaP).

A large volume of work points to the plasticity of tissue macrophages that are educated by tumor environmental cues to promote tumor growth (8). Hence, we interrogated whether irradiation could skew bone marrow-derived macrophages (BMDM) towards the gene expression profiles of pro-tumorigenic macrophages. Direct irradiation with 3 Gy (Fig 3B) and indirect effects transmitted through co-culturing BMDM with irradiated tumor-conditioned media (Fig 3C) both polarized BMDM towards a pro-tumorigenic phenotype, as we observed increased expression of Arg1, Fizz, IL-1β, IL-10, MMP-9, VEGF-A, CD206 and CSF1, and decreased expression of inflammatory genes such as iNOS and IL-12. As a reflection of their immunosuppressive roles in tumors, protumorigenic macrophages also typically exhibit lower MHCII expression (28). By FACS analysis, all (100%) of the $CD11b^{+}F4/80^{+}$ macrophages from irradiated tumors displayed low MHCII expression, while only 50% of the macrophages in non-irradiated tumors were $MHCII^{low}$ (Fig 3D). These data suggest that both direct and indirect effects of irradiation can have profound effects on macrophages by skewing them towards a protumorigenic subtype with enhanced migration ability and gene expression profile that favor tumor growth.

CSF1 expression is increased by irradiation

Next, we examined whether tumor cell irradiation can alter the expression of cytokines known to participate in myeloid cell recruitment (6, 29). The expression of CSF1, CCL2, CCL5 and SDF-1 was examined in Myc-CaP cells 24hrs after 3Gy of irradiation. Among these cytokines examined, CSF1 showed the highest expression and the most significant increase in irradiated over untreated tumor cells (Fig 4A). We further evaluated secreted levels of CSF1 protein, which was elevated in conditioned media from irradiated tumor cells (Fig 4B). IL-34 is a recently discovered second CSF1R ligand that functions similarly to CSF1 (30). However the expression of IL-34 was 100 fold lower than CSF1 in our two prostate cancer systems (RM-1 and Myc-CaP model, data not shown), and thus, we did not pursue IL-34 further. The ability of irradiation to augment CSF1 expression appeared to be a general phenomenon. In total, we tested 9 murine and human cancer cell lines, 8 out of 9

showed an increase in CSF1 after irradiation (Fig 4A, Fig 4E, Supplemental Fig 3). Consistent with results from cell culture experiments, irradiated tumors (the same cohort as Fig 1A) showed a significant increase in CSF1 gene expression compared to untreated tumors (Fig 4C). Importantly, an increase in CSF1 was also observed in the serum of prostate cancer patients after radiotherapy (Fig 4D), supporting the clinical relevance of CSF1 increase seen in our murine models.

To explore the issue of crosstalk between tumor cells and macrophages on the CSF1 axis, we co-cultured RAW264.7 macrophages or bone marrow derived macrophages (BMDM) with RM-1 tumor cells and observed an increase in the magnitude of CSF1 expression above that in either cell grown alone, especially in the irradiation setting (Fig 4E and F). Furthermore, the addition of a highly selective CSF1R kinase inhibitor GW2850 (31) resulted in a complete negation of increased macrophage migration towards irradiated tumor-conditioned media (Figure 4G). Collectively, these data demonstrate that irradiation increases CSF1 expression in tumors, which is amplified by tumor-macrophage interactions. The heightened CSF1 production induced by irradiation in turn drives macrophage migration and recruitment into irradiated tumors.

Irradiation enhances CSF1 production through an ABL1-dependent mechanism

Given our finding shown above that irradiation boosts tumoral CSF1 expression, we sought to interrogate a signal transduction pathway implicated in irradiation -induced transcriptional regulation of CSF1. ABL1, a non-receptor tyrosine kinase, is known for mediating apoptosis and cycle arrest after irradiation (32). It has been reported that ABL1 can also be recruited to the promoter region of CSF1 and regulates CSF1 gene expression in concert with AP-1 (33). Thus, we examined in detail the kinetics of irradiation-induced CSF1 expression and ABL1 activation in our system. First, detailed analysis of irradiation-induced gene expression of CSF1 in Myc-CaP cells showed the increase in CSF1 RNA initiated at 4 hr post irradiation (Fig 5A). Next we profiled the activation of ABL1 protein in response to irradiation. We observed that two ABL1 cleavage products, 75kD and 60kD product, emerged 2hr post irradiation (Fig 5B). Further examination of the subcellular localization of ABL1 by confocal microscopy revealed that prior to the radiation insult, ABL1 was predominantly located in the cytoplasm with very little ABL1 immunocytochemical signal registered in the nucleus (Fig 5C, left). As early as 1hr after irradiation a noticeable portion but not all of the ABL1 protein has translocated to the nucleus (Fig 5C, middle), and this is maintained at 4hr (Fig 5C, right). To further substantiate the functional impact of ABL1 on the CSF1 gene expression, we analyzed the binding of ABL1 to the CSF1 promoter by a chromatin immunoprecipitation assay (ChIP). An increase in ABL1 binding to the CSF1 promoter was observed as early as 1hr after irradiation and peaked at 2hrs before slowly declining (Fig 5D). When looking into the kinetics of RNA polymerase II binding to the CSF1 promoter, it first showed a significant decrease at 1hr and an increase starting 2hrs post irradiation (Fig 5E). This bell shape kinetics of RNA polymerase activity could be attributed to the radiation-induced DNA damage causing an initial inhibition on transcription (34). The timing of ABL1 nuclear translocation, its binding to the CSF1 promoter, and the binding of RNA polymerase II to

the CSF1 promoter preceded the changes in CSF1 mRNA level. These findings support the involvement of ABL1 in the regulation of CSF1 expression in response to irradiation.

Next, we used an ABL1-targeted siRNA and small molecular inhibitor to further confirm its regulatory role on CSF1 in our system. The irradiation induced CSF1 expression in MycCaP cells was significantly inhibited by the addition of the ABL1 kinase inhibitor, STI-571 (5 μM, Fig 5F). A similar result was also observed in the human prostate cancer cell line CWR22Rv1 (Supplemental Fig 4A). Using a migration assay, we found that STI-571-treated conditioned media displayed decreased ability to promote macrophage migration (Fig 5G). Furthermore, the addition of GW2580 to macrophages (top chamber) did not further retard macrophage migration over STI treatment of tumor cells (Fig 5G), suggesting STI-571 and GW2580 may be targeting the same pathway to regulate migration. Like most of the pharmacologic protein kinase inhibitors, STI-571 is not completely specific. STI-571 also inhibits c-Kit, platelet-derived growth factor receptor (PDGFR) and CSF1R (35). Thus, we employed siRNA-mediated knockdown of ABL1 to examine its effect on CSF1. Due to the low efficiency of transfecting murine prostate cancer cells, we used the human CWR22Rv1 cell line for this experiment. The ABL1 siRNA was able to decrease ABL1 mRNA expression to 30% of the normal level in the CWR22Rv1 cells (Fig 5H, right panel). As expected, ABL1 siRNA effectively blocked the CSF1 mRNA induction by irradiation (Fig 5H, left panel). These data suggest that upon irradiation, ABL1 is activated, translocates to the nucleus, binds to the promoter region of CSF1 and promotes its expression.

Blockade of CSF1/CSF1R signaling retards tumor regrowth after local irradiation

CSF1 is a potent cytokine well-known to promote myeloid cell proliferation, differentiation and migration. In a recent study, we demonstrated that blockade of CSF1/CSF1R signaling can effectively inhibit TIM function and recruitment to tumors (15). Thus, in this study we investigated whether blocking CSF1R can also reduce TIMs recruitment and diminish their pro-tumorigenic influences in the RT setting. The combined irradiation and CSF1R blockade treatment was first tested with the selective CSF1R inhibitor, GW2580. Significant reductions in TIM populations in RM-1 tumors were observed with GW2580 treatment (160mg/kg/day), which augmented the efficacy of irradiation by achieving more effective suppression of tumor growth than irradiation alone (supplemental Fig 5A–E, and data not shown). To further substantiate this rational combination strategy, we employed a recently described small molecule, CSF1R kinase inhibitor PLX3397. This inhibitor was shown to be a highly potent inhibitor of CSF1R (cFMS) with IC_{50} of 20nM and it is under active clinical investigation for several types of cancers (19). Here, RM-1 prostate tumor bearing mice were treated with control (chow), local irradiation (3Gy×5 days), PLX3397 (drug chow) or the combination. As shown in Figure 6A, PLX3397 alone has little effect on tumor growth compared with the control group. Irradiation reduced tumor size by 43% at day 10, 1 day after cessation of irradiation ($p<0.001$). The irradiated tumor sizes were stabilized for a short duration, and subsequently resumed an aggressive tumor growth rate, whereas the combined irradiation and PLX3397 treated group maintained a much slower growth rate (Fig 6A). Both flow cytometry and histological analyses of tumors revealed a significant reduction of $CD11b^+Gr\text{-}1^+$ MDSCs and $CD11b^+F4/80^+$ macrophages in tumors as well as in spleens of both PLX3397-treated groups, with more pronounced effects observed in the combination

treatment (Fig 6B–E, and G). Interestingly, both subsets of MDSCs, monocytic and polymorphonuclear, were reduced by PLX3397 (Fig 6F), a result that differed from our previous findings with GW2580 treatment in 3LL tumors where only the monocytic subtype of MDSCs was inhibited (15). At the molecular level, CSF1R blockade significantly reduced RT-induced CSF1, MMP9 and Arg1 (Fig 6 H–J). The latter 2 genes are known to be involved in cancer progression and metastasis by promoting tissue remodeling, angiogenesis, and immunosuppression (15). Similar reductions in the expression of CSF1 and Arg1 were also observed in irradiated tumors treated with GW2580, along with a significant reduction in the macrophage chemotactic factor, CCL2 (Supplemental Fig 5D–E). In summary, we observed that prostate tumor-directed irradiation can potently induce the influx of TIMs, which in turn can thwart treatment efficacy. The addition of potent CSF1R inhibitors such as PLX3397 and GW2580 can prevent the influx of TIMs and halt their pro-tumorigenic functions leading to more effective and durable tumor growth control.

Discussion

In the present study, we demonstrate that the recruitment of TIMs to prostate tumors is highly induced by local irradiation in several immunocompetent mouse models. We find elevated expression of CSF1, an important cytokine for macrophage survival, migration and differentiation, in tumor cells after irradiation, which was also observed in the serum of post-radiotherapy prostate cancer patients. Increased CSF1 expression was mediated, at least partially, by the ABL1 tyrosine kinase. Upon irradiation, ABL1 was activated and translocated to the nucleus, where it bound to the promoter region of CSF1 to up-regulate its expression. We further showed that blockade of CSF1R with selective small molecule kinase inhibitors, such as GW2580and PLX3397, greatly inhibit TIMs infiltration and significantly delay tumor re-growth after irradiation. These results suggest that disrupting the pro-tumorigenic contributions of host innate immune cells, namely MDSCs and macrophages, through blockade of the CSF1/CSF1R axis can be a promising approach for developing rational and more effective combination cancer therapies. A schema of irradiation induced expression of CSF1 and recruitment of TIMs and the impact of CSF1R inhibition on TIMs' modulation of tumor regrowth is shown in Figure 7.

The use of immunocompetent murine prostate tumor models in this study allowed us to directly assess the contributions of host immune cells, in particular the distinct myeloid subpopulations, to tumor progression after therapy. Our results demonstrated that the major impact of CSF1R blockade is directed at the tumor microenvironment, namely TIMs. Interestingly, CSF1R has been shown to be expressed and can contribute to the oncogenesis of several types of cancer, including prostate cancer (36, 37). Hence, the blockade of the CSF1/CSF1R axis could potentially have a direct suppressive impact on tumor cells, albeit unlikely as the the RM-1 and Myc-CaP tumors used here express negligible levels of CSF1R based on sensitive RT-PCR analyses (data not shown). We also believe IL-34, a newly identified ligand for CSF1R having similar functions in stimulating macrophage proliferation and migration (30, 38), is unlikely to play a significant role as its expression level is 100-fold lower than CSF1 in our models(data not shown). Recent findings from Dr. Hong Wu's group using the PTEN-knockout transgenic prostatic carcinoma model revealed that intratumoral MDSCs expansion contributes to tumor progression and that CSF1R

blockade was an effective means to suppress the infiltration and function of MDSCs in this spontaneous murine prostate cancer model (data not shown).

It is promising that our initial exploratory study on 10 consecutive prostate cancer patients, who recently underwent RT, also yielded data supportive of CSF1 axis being involved. Although our data suggests that serum CSF1 could potentially be a biomarker of TIMs recruitment, there are several considerations that caution against this premature conclusion. First, a wide range of serum CSF1 level was detected in patients (Figure 4D). This issue could likely be attributed to the different infection or inflammation status of the patients. Second, the timing of patient specimen procurement after RT was not uniform between patients in the small cohort tested. We did observe an increase in a MDSC population ($CD11b^{+}CD15^{+}$) in the peripheral blood of a few patients whose serum CSF1 increased from pre- to post-RT (data not shown). Due to the heterogeneity issues, data from a much larger cohort of patients will be needed to fully validate the concept put forth here. We are actively pursuing these studies with more and standardized time points of peripheral blood collection in prostate cancer patients undergoing RT.

Our findings are consistent with CSF1 being an important stimulus for the influx of TIMs to tumors especially in response to irradiation. However, our study does not exclude other pathways that may also be involved in this complex inflammatory cascade. For instance, several recent papers highlighted the role of the SDF-1/CXCR4 axis in local irradiation-induced influx of TIMs to tumors (5, 6). The authors demonstrated that irradiation-induced hypoxia though destruction of endothelial cells and the microvasculature, and the resultant increased expression of HIF-1α in turn induced the expression of CXCR4 and SDF-1, which then mediated the recruitment of TIMs to tumors. Likewise, CCL2 has also been implicated in the recruitment of bone marrow-derived myeloid cells into tumors and this axis can also modulate prostate cancer growth and metastasis to bone (39) (40). However, we observed negligible SDF-1 and CCL2 expression with or without irradiation in our tumor cells (Fig 4A). The migration/recruitment of TIMs is a complex process that is likely regulated by several pathways, especially in the context of different tumor types, host genetic background and stimulus induced by different therapeutic settings or progression status. Of interest, we consistently observed a decrease in CCL2 level with GW2580 or PLX3397 treatment (data not shown and supplemental data Fig 5F). This finding is also in accordance with a recent study which showed the removal of CSF1 significantly decreases CCL2 (41). An intriguing possibility could be that CSF1 is an upstream regulator of other cytokines like CCL2. Clearly the influence of CSF1/CSF1R axis and its cross-talk with other cytokine/chemokine pathways in the recruitment of TIMs deserves further investigation.

A unique aspect of this study is the finding that the ABL1 pathway mediates the heightened CSF1 transcription induced by irradiation. Several factors have been implicated in the regulation of CSF1 gene expression, including PDGF (42), ABL1 (33), Interferon-Gamma (43) and AP-1, CTF/NF-1, SP1, SP3 (44) and nuclear actin (45) in different cell types and contexts. Among these, ABL1 is known to respond to irradiation or DNA damage via DNA-PK, ATM and p53 pathway (46–48). ABL1 contains a catalytic domain as well as a NES and three NLS motifs. Several groups reported that ABL1 localizes to both nucleus and cytoplasm and can shuttle between these two compartments (49). In our study, we observed

that a portion of cytoplasmic ABL1 is activated and translocated to the nucleus as early as 1hr after irradiation (Fig 5B). The ABL1 DNA-binding domain is critical for its biological function (50), yet no classical DNA-binding motifs have been identified so far. The few ABL1 transcriptional targets identified include p21 and CSF1 (33, 51). Here we demonstrated that ABL1 binds to the promoter region of CSF1 and activates CSF1 gene transcription. A previous study suggested that ABL1 forms a complex with AP-1, a transcription factor composed of c-jun and c-fos, in the regulation of CSF1 (33). Based on this finding, a potential feedback loop in CSF1R-dependent cells is that the blockade of CSF1R signaling inhibits c-fos, which further downregulates CSF1 expression. This mechanism might explain why we observed a decrease in CSF1 expression in tumors after PLX3397 treatment (Figure 6H).

In summary, the data presented in this study demonstrates that irradiation induces CSF1 through an ABL1-dependent mechanism in prostate cancer. The heightened CSF1 serves a critical role in the systemic recruitment of pro-tumorigenic myeloid cells to irradiated tumors. Hence, the blockade of TIMs in combination with local irradiation of prostate tumors displays an augmented and more durable response than irradiation alone in preclinical models. We believe that co-targeting the CSF1/CSF1R pathway with local irradiation of prostate tumors will be a promising strategy for clinical translation.

Supplementary Material

Refer to Web version on PubMed Central for supplementary material.

Acknowledgments

We are grateful to Drs. Steven Bensinger, John Colicelli and Arnie Berk for helpful discussions. This work was supported by DOD CDMRP W81XWH-12-1-0206 (to LW), NCI SPORE P50 CA092131, and Margaret E. Early Medical Trust award (to LW). We thank UCLA JCCC and UCLA CTSI (1UL1RR033176) respectively for providing postdoctoral fellowship support to JX and translational infrastructural services.

Abbreviations

BMDM	bone marrow derived macrophage
CSF	colony stimulating factor
CML	chronic myelogenous leukemia
DAPI	4,6-diamidino-2-phenylindole
DMEM	Dulbecco modified eagle medium
FBS	fetal bovine serum
RBC	red blood cell
TAM	tumor-associated macrophage
TIM	tumor infiltrating myeloid cells
MDSC	myeloid-derived suppressor cell

MO-MDSC	mononuclear-MDSC
PMN-MDSC	polymorphonuclear-MDSC
MMP	matrix metalloproteinase

References

1. Delaney G, Jacob S, Featherstone C, Barton M. The role of radiotherapy in cancer treatment: estimating optimal utilization from a review of evidence-based clinical guidelines. Cancer. 2005; 104(6):1129–1137. Epub 2005/08/05. PubMed PMID:16080176. [PubMed: 16080176]
2. Agarwal PK, Sadetsky N, Konety BR, Resnick MI, Carroll PR. Treatment failure after primary and salvage therapy for prostate cancer: likelihood, patterns of care, and outcomes. Cancer. 2008; 112(2):307–314. Epub 2007/12/01. PubMed PMID:18050294. [PubMed: 18050294]
3. D'Amico AV, Renshaw AA, Sussman B, Chen MH. Pretreatment PSA velocity and risk of death from prostate cancer following external beam radiation therapy. Jama. 2005; 294(4):440–447. Epub 2005/07/28. PubMed PMID:16046650. [PubMed: 16046650]
4. Bianco FJ Jr, Scardino PT, Stephenson AJ, Diblasio CJ, Fearn PA, Eastham JA. Long-term oncologic results of salvage radical prostatectomy for locally recurrent prostate cancer after radiotherapy. Int J Radiat Oncol Biol Phys. 2005; 62(2):448–453. Epub 2005/05/14. PubMed PMID:15890586. [PubMed: 15890586]
5. Kozin SV, Kamoun WS, Huang Y, Dawson MR, Jain RK, Duda DG. Recruitment of myeloid but not endothelial precursor cells facilitates tumor regrowth after local irradiation. Cancer Res. 2010; 70(14):5679–5685. Epub 2010/07/16. PubMed PMID:20631066; PubMed Central PMCID: PMC2918387. [PubMed: 20631066]
6. Kioi M, Vogel H, Schultz G, Hoffman RM, Harsh GR, Brown JM. Inhibition of vasculogenesis, but not angiogenesis, prevents the recurrence of glioblastoma after irradiation in mice. J Clin Invest. 2010; 120(3):694–705. Epub 2010/02/25. PubMed PMID:20179352; PubMed Central PMCID: PMC2827954. [PubMed: 20179352]
7. Hanahan D, Coussens LM. Accessories to the crime: functions of cells recruited to the tumor microenvironment. Cancer cell. 2012; 21(3):309–322. Epub 2012/03/24. PubMed PMID:22439926. [PubMed: 22439926]
8. Qian BZ, Pollard JW. Macrophage diversity enhances tumor progression and metastasis. Cell. 2010; 141(1):39–51. Epub 2010/04/08.. PubMed PMID:20371344. [PubMed: 20371344]
9. Shojaei F, Wu X, Malik AK, Zhong C, Baldwin ME, Schanz S, et al. Tumor refractoriness to anti-VEGF treatment is mediated by CD11b+Gr1+ myeloid cells. Nat Biotechnol. 2007; 25(8):911–920. Epub 2007/08/01. PubMed PMID:17664940. [PubMed: 17664940]
10. Muthana M, Rodrigues S, Chen YY, Welford A, Hughes R, Tazzyman S, et al. Macrophage Delivery of an Oncolytic Virus Abolishes Tumor Regrowth and Metastasis After Chemotherapy or Irradiation. Cancer Res. 2012 PubMed PMID:23172310.
11. Murdoch C, Muthana M, Coffelt SB, Lewis CE. The role of myeloid cells in the promotion of tumour angiogenesis. Nat Rev Cancer. 2008; 8(8):618–631. Epub 2008/07/18. PubMed PMID: 18633355. [PubMed: 18633355]
12. Lewis CE, Pollard JW. Distinct role of macrophages in different tumor microenvironments. Cancer research. 2006; 66(2):605–612. Epub 2006/01/21. PubMed PMID:16423985. [PubMed: 16423985]
13. Ostrand-Rosenberg S, Sinha P. Myeloid-derived suppressor cells: linking inflammation and cancer. J Immunol. 2009; 182(8):4499–4506. Epub 2009/04/04. PubMed PMID:19342621; PubMed Central PMCID: PMC2810498. [PubMed: 19342621]
14. Gabrilovich DI, Nagaraj S. Myeloid-derived suppressor cells as regulators of the immune system. Nat Rev Immunol. 2009; 9(3):162–174. Epub 2009/02/07. PubMed PMID:19197294;PubMed Central PMCID: PMC2828349. [PubMed: 19197294]

15. Priceman SJ, Sung JL, Shaposhnik Z, Burton JB, Torres-Collado AX, Moughon DL, et al. Targeting distinct tumor-infiltrating myeloid cells by inhibiting CSF-1 receptor: combating tumor evasion of antiangiogenic therapy. Blood. 2010; 115(7):1461–1471. Epub 2009/12/17. PubMed PMID:20008303; PubMed Central PMCID: PMC2826767. [PubMed: 20008303]
16. Yang L, DeBusk LM, Fukuda K, Fingleton B, Green-Jarvis B, Shyr Y, et al. Expansion of myeloid immune suppressor Gr+CD11b+ cells in tumor-bearing host directly promotes tumor angiogenesis. Cancer Cell. 2004; 6(4):409–421. Epub 2004/10/19. PubMed PMID:15488763. [PubMed: 15488763]
17. Hamilton JA. Colony-stimulating factors in inflammation and autoimmunity. Nat Rev Immunol. 2008; 8(7):533–544. Epub 2008/06/14. PubMed PMID:18551128. [PubMed: 18551128]
18. Chitu V, Stanley ER. Colony-stimulating factor-1 in immunity and inflammation. Curr Opin Immunol. 2006; 18(1):39–48. Epub 2005/12/13. PubMed PMID:16337366. [PubMed: 16337366]
19. DeNardo D, Brennan DJ, Rexhepaj E, Ruffell B, Shiao SL, Madden SF, et al. Leukocyte complexity predicts breast cancer survival and functionally regulates response to chemotherapy. Cancer Discovery. 2011; 1:52–65.
20. Wang JY. Nucleo-cytoplasmic communication in apoptotic response to genotoxic and inflammatory stress. Cell Res. 2005; 15(1):43–48. Epub 2005/02/03. PubMed PMID:15686626. [PubMed: 15686626]
21. Ren X, Xu J, Cooper JP, Kang MH, Erdreich-Epstein A. c-Abl is an upstream regulator of acid sphingomyelinase in apoptosis induced by inhibition of integrins alphavbeta3 and alphavbeta5. PLoS One. 2012; 7(8):e42291. Epub 2012/08/11. PubMed PMID:22879933; PubMed Central PMCID: PMC3411766. [PubMed: 22879933]
22. Xu J, Millard M, Ren X, Cox OT, Erdreich-Epstein A. c-Abl mediates endothelial apoptosis induced by inhibition of integrins alphavbeta3 and alphavbeta5 and by disruption of actin. Blood. 2010; 115(13):2709–2718. Epub 2010/02/04. PubMed PMID:20124512; PubMed Central PMCID: PMC2852370. [PubMed: 20124512]
23. Ogawa Y, Kawamura T, Furuhashi M, Tsukamoto K, Shimada S. Improving chemotherapeutic drug penetration in melanoma by imatinib mesylate. J Dermatol Sci. 2008; 51(3):190–199. Epub 2008/05/20. PubMed PMID:18485676. [PubMed: 18485676]
24. Ganguly SS, Fiore LS, Sims JT, Friend JW, Srinivasan D, Thacker MA, et al. c-Abl and Arg are activated in human primary melanomas, promote melanoma cell invasion via distinct pathways, and drive metastatic progression. Oncogene. 2011 Epub 2011/09/06. PubMed PMID:21892207; PubMed Central PMCID: PMC3235241.
25. Srinivasan D, Sims JT, Plattner R. Aggressive breast cancer cells are dependent on activated Abl kinases for proliferation, anchorage-independent growth and survival. Oncogene. 2008; 27(8): 1095–1105. Epub 2007/08/19. PubMed PMID:17700528. [PubMed: 17700528]
26. Baley PA, Yoshida K, Qian W, Sehgal I, Thompson TC. Progression to androgen insensitivity in a novel in vitro mouse model for prostate cancer. J Steroid Biochem Mol Biol. 1995; 52(5):403–413. Epub 1995/05/01. PubMed PMID:7538321. [PubMed: 7538321]
27. Youn JI, Nagaraj S, Collazo M, Gabrilovich DI. Subsets of myeloid-derived suppressor cells in tumor-bearing mice. Journal of immunology. 2008; 181(8):5791–5802. Epub 2008/10/04. PubMed PMID:18832739; PubMed Central PMCID: PMC2575748.
28. Gordon S. Alternative activation of macrophages. Nature reviews Immunology. 2003; 3(1):23–35. Epub 2003/01/04. PubMed PMID:12511873.
29. Murdoch C, Giannoudis A, Lewis CE. Mechanisms regulating the recruitment of macrophages into hypoxic areas of tumors and other ischemic tissues. Blood. 2004; 104(8):2224–2234. Epub 2004/07/03. PubMed PMID:15231578. [PubMed: 15231578]
30. Lin H, Lee E, Hestir K, Leo C, Huang M, Bosch E, et al. Discovery of a cytokine and its receptor by functional screening of the extracellular proteome. Science. 2008; 320(5877):807–811. Epub 2008/05/10. PubMed PMID:18467591. [PubMed: 18467591]
31. Conway JG, McDonald B, Parham J, Keith B, Rusnak DW, Shaw E, et al. Inhibition of colony-stimulating-factor-1 signaling in vivo with the orally bioavailable cFMS kinase inhibitor GW2580. Proc Natl Acad Sci U S A. 2005; 102(44):16078–16083. Epub 2005/10/27. PubMed PMID: 16249345; PubMed Central PMCID: PMC1276040. [PubMed: 16249345]

32. Yuan ZM, Huang Y, Ishiko T, Kharbanda S, Weichselbaum R, Kufe D. Regulation of DNA damage-induced apoptosis by the c-Abl tyrosine kinase. Proceedings of the National Academy of Sciences of the United States of America. 1997; 94(4):1437–1440. Epub 1997/02/18. PubMed PMID:9037071; PubMed Central PMCID: PMC19809. [PubMed: 9037071]

33. Chen C, Shang X, Cui L, Xu T, Luo J, Ba X, et al. L-selectin ligation-induced CSF-1 gene transcription is regulated by AP-1 in a c-Abl kinase-dependent manner. Hum Immunol. 2008; 69(8):501–509. Epub 2008/07/16. PubMed PMID:18619508. [PubMed: 18619508]

34. Rockx DA, Mason R, van Hoffen A, Barton MC, Citterio E, Bregman DB, et al. UV-induced inhibition of transcription involves repression of transcription initiation and phosphorylation of RNA polymerase II. Proceedings of the National Academy of Sciences of the United States of America. 2000; 97(19):10503–10508. Epub 2000/09/06. PubMed PMID:10973477; PubMed Central PMCID: PMC27054. [PubMed: 10973477]

35. Dewar AL, Cambareri AC, Zannettino AC, Miller BL, Doherty KV, Hughes TP, et al. Macrophage colony-stimulating factor receptor c-fms is a novel target of imatinib. Blood. 2005; 105(8):3127–3132. Epub 2005/01/08. PubMed PMID:15637141. [PubMed: 15637141]

36. Ide H, Seligson DB, Memarzadeh S, Xin L, Horvath S, Dubey P, et al. Expression of colony-stimulating factor 1 receptor during prostate development and prostate cancer progression. Proceedings of the National Academy of Sciences of the United States of America. 2002; 99(22): 14404–14409. Epub 2002/10/17. PubMed PMID:12381783; PubMed Central PMCID: PMC137896. [PubMed: 12381783]

37. Wrobel CN, Debnath J, Lin E, Beausoleil S, Roussel MF, Brugge JS. Autocrine CSF-1R activation promotes Src-dependent disruption of mammary epithelial architecture. J Cell Biol. 2004; 165(2): 263–273. Epub 2004/05/01. PubMed PMID:15117969; PubMed Central PMCID: PMC2172030. [PubMed: 15117969]

38. Wei S, Nandi S, Chitu V, Yeung YG, Yu W, Huang M, et al. Functional overlap but differential expression of CSF-1 and IL-34 in their CSF-1 receptor-mediated regulation of myeloid cells. J Leukoc Biol. 2010; 88(3):495–505. Epub 2010/05/28. PubMed PMID:20504948; PubMed Central PMCID: PMC2924605. [PubMed: 20504948]

39. Sawanobori Y, Ueha S, Kurachi M, Shimaoka T, Talmadge JE, Abe J, et al. Chemokine-mediated rapid turnover of myeloid-derived suppressor cells in tumor-bearing mice. Blood. 2008; 111(12): 5457–5466. Epub 2008/04/01. PubMed PMID:18375791. [PubMed: 18375791]

40. Li X, Loberg R, Liao J, Ying C, Snyder LA, Pienta KJ, et al. A destructive cascade mediated by CCL2 facilitates prostate cancer growth in bone. Cancer research. 2009; 69(4):1685–1692. Epub 2009/01/30. PubMed PMID:19176388; PubMed Central PMCID: PMC2698812. [PubMed: 19176388]

41. El Chartouni C, Benner C, Eigner M, Lichtinger M, Rehli M. Transcriptional effects of colony-stimulating factor-1 in mouse macrophages. Immunobiology. 2010; 215(6):466–474. Epub 2009/09/18. PubMed PMID:19758725. [PubMed: 19758725]

42. Wittrant Y, Bhandari BS, Abboud H, Benson N, Woodruff K, MacDougall M, et al. PDGF up-regulates CSF-1 gene transcription in ameloblast-like cells. J Dent Res. 2008; 87(1):33–38. Epub 2007/12/22. PubMed PMID:18096890. [PubMed: 18096890]

43. Tsuchimoto D, Tojo A, Asano S. A mechanism of transcriptional regulation of the CSF-1 gene by interferon-gamma. Immunol Invest. 2004; 33(4):397–405. Epub 2004/12/31. PubMed PMID: 15624698. [PubMed: 15624698]

44. Harrington M, Konicek BW, Xia XL, Song A. Transcriptional regulation of the mouse CSF-1 gene. Mol Reprod Dev. 1997; 46(1):39–44. discussion-5. Epub 1997/01/01. PubMed PMID: 8981362. [PubMed: 8981362]

45. Song Z, Wang M, Wang X, Pan X, Liu W, Hao S, et al. Nuclear actin is involved in the regulation of CSF1 gene transcription in a chromatin required, BRG1 independent manner. J Cell Biochem. 2007; 102(2):403–411. Epub 2007/03/30. PubMed PMID:17393431. [PubMed: 17393431]

46. Hamer G, Gademan IS, Kal HB, de Rooij DG. Role for c-Abl and p73 in the radiation response of male germ cells. Oncogene. 2001; 20(32):4298–4304. Epub 2001/07/24. PubMed PMID: 11466610. [PubMed: 11466610]

47. Kharbanda S, Bharti A, Pei D, Wang J, Pandey P, Ren R, et al. The stress response to ionizing radiation involoves c-Abl-dependent phosphorylation of SHPTP1. Proceedings of the National

Academy of Sciences of the United States of America. 1996; 93(14):6898–6901. Epub 1996/07/09. PubMed PMID:8692915; PubMed Central PMCID: PMC38905. [PubMed: 8692915]

48. Baskaran R, Wood LD, Whitaker LL, Canman CE, Morgan SE, Xu Y, et al. Ataxia telangiectasia mutant protein activates c-Abl tyrosine kinase in response to ionizing radiation. Nature. 1997; 387(6632):516–519. Epub 1997/05/29. PubMed PMID:9168116. [PubMed: 9168116]
49. Lewis JM, Baskaran R, Taagepera S, Schwartz MA, Wang JY. Integrin regulation of c-Abl tyrosine kinase activity and cytoplasmic-nuclear transport. Proceedings of the National Academy of Sciences of the United States of America. 1996; 93(26):15174–15179. Epub 1996/12/24. PubMed PMID:8986783; PubMed Central PMCID: PMC26376. [PubMed: 8986783]
50. Kipreos ET, Wang JY. Cell cycle-regulated binding of c-Abl tyrosine kinase to DNA. Science. 1992; 256(5055):382–385. Epub 1992/04/17. PubMed PMID:1566087. [PubMed: 1566087]
51. Jing Y, Wang M, Tang W, Qi T, Gu C, Hao S, et al. c-Abl tyrosine kinase activates p21 transcription via interaction with p53. J Biochem. 2007; 141(5):621–626. Epub 2007/03/07. PubMed PMID:17339230. [PubMed: 17339230]

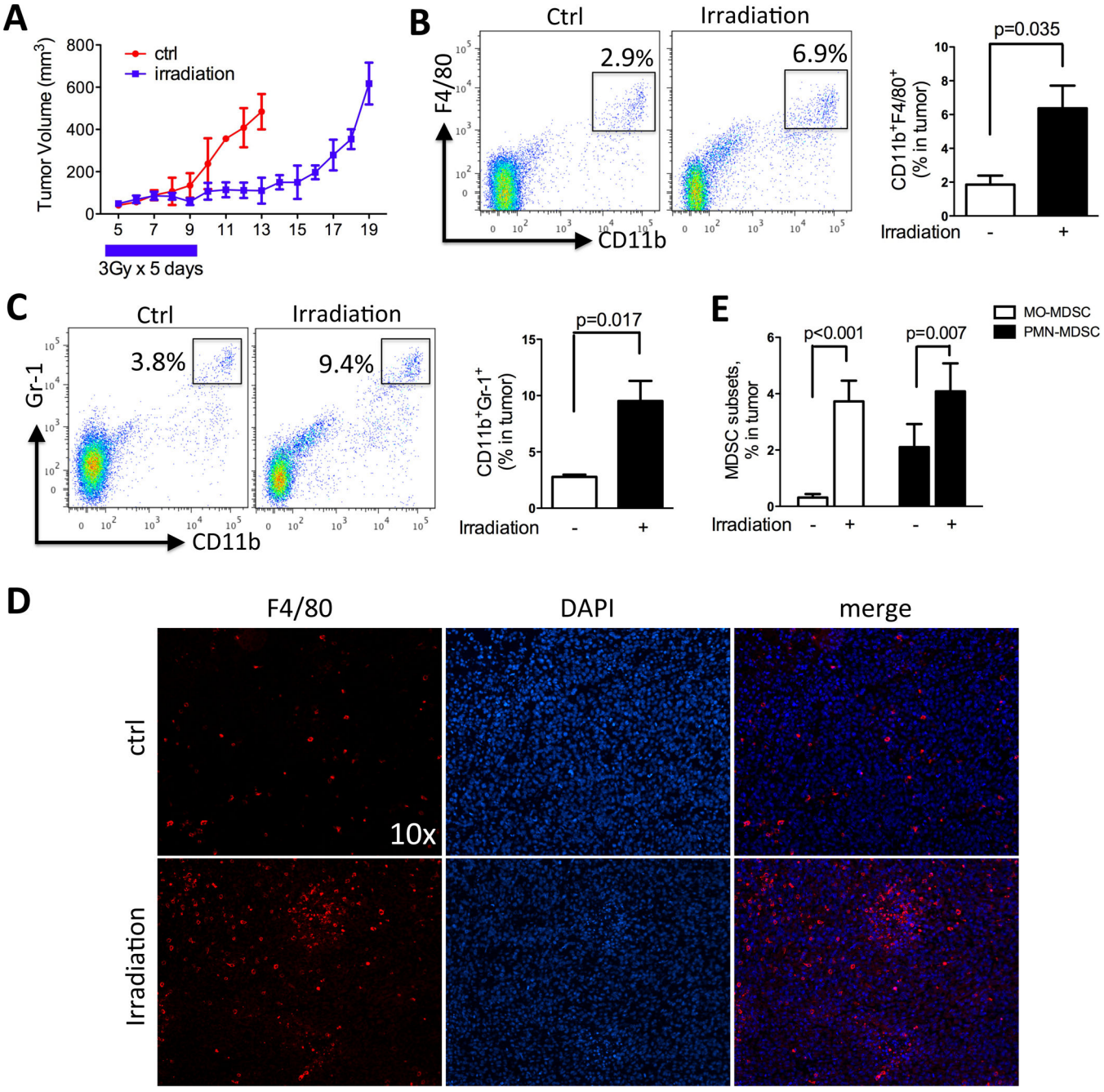

Figure 1. Local irradiation enhances myeloid infiltration into tumors

Subcutaneous RM-1 tumors were collected, processed to single cell suspension and assayed by FACS and immunohistochemistry for $CD11b^+Gr\text{-}1^+$ MDSCs and $CD11b^+F4/80^+$ TAMs. A) Growth curve of RM-1 tumors with or without irradiation. B) FACS plots and quantification of TAMs in tumor. C) FACS plots and quantification for MDSCs in tumor. D) Representative F4/80 staining of RM-1 tumors from control and irradiation-treated mice. E) Effect of irradiation on the two subsets of MDSCs: MO-MDSC and PMN-MDSC. N=4 for each group.

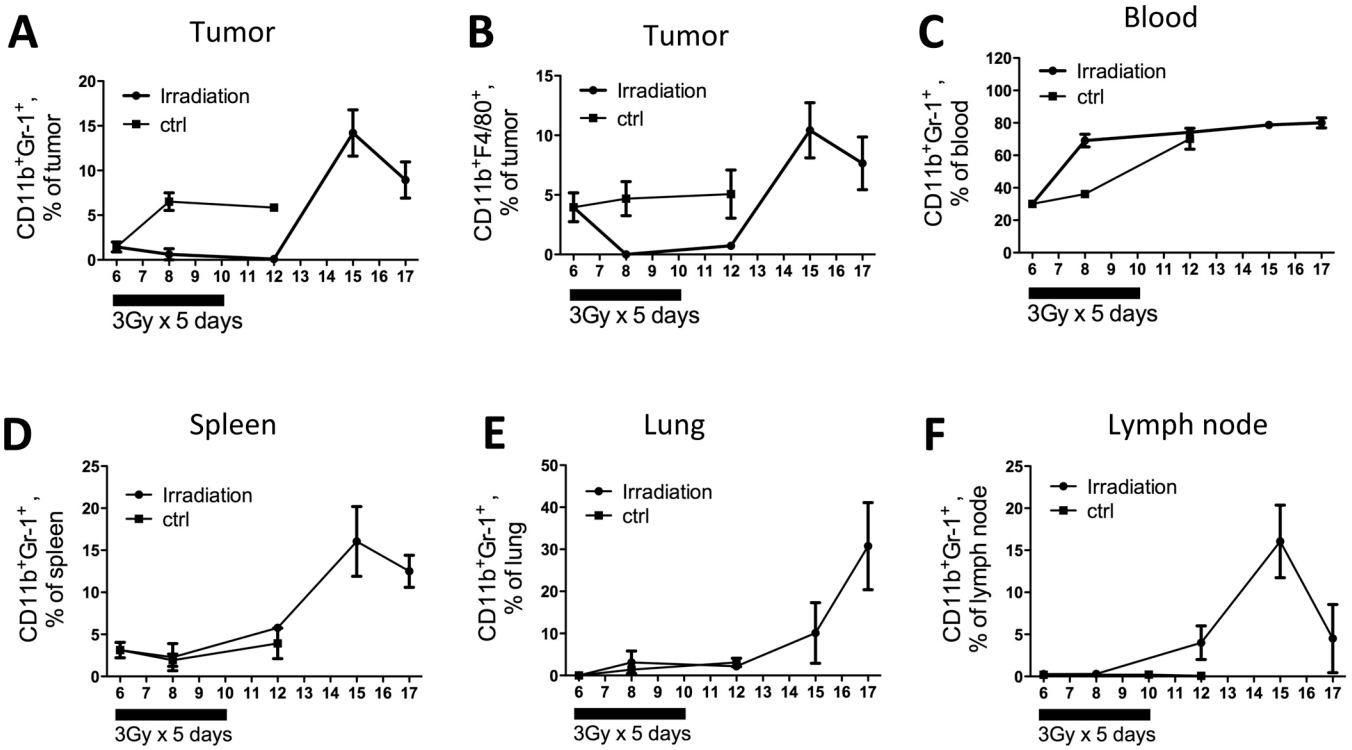

Figure 2. Local irradiation enhances systemic myeloid cell expansion

Control mice were sacrifice on day 6, 8 and 12. Irradiated mice were sacrificed on day 6, 8, 12, 15 and 17. Tumors, blood, spleens, lungs and lymph nodes were collected for FACS analysis for MDSC and TAM population. N=4 for each time point.

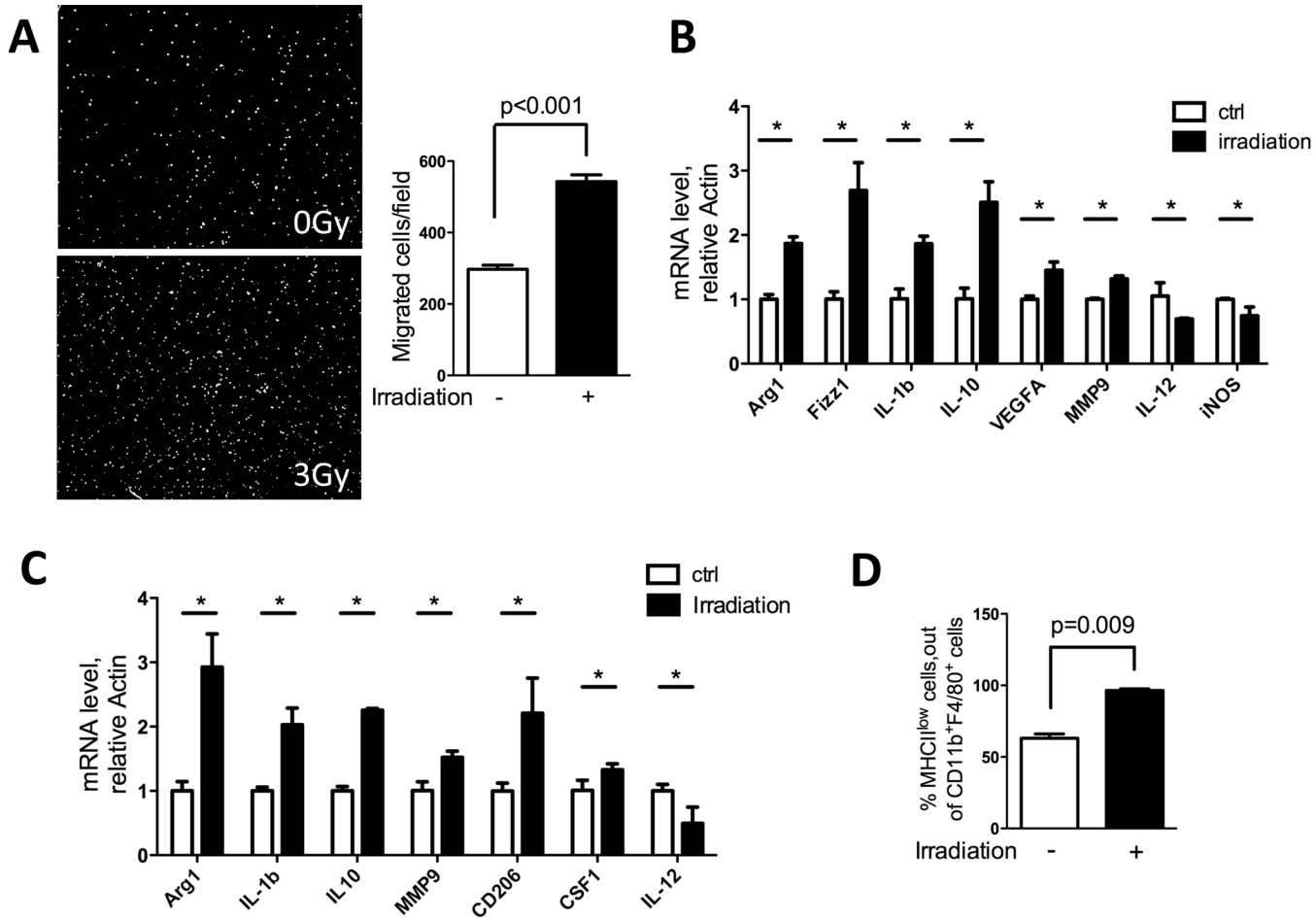

Figure 3. Irradiation increases cell migration and induces protumorigenic genes in macrophages

A) RAW264.7 macrophages were seeded in 8-μm transwell inserts, and tumor conditioned media (collected 48hrs after 3Gy irradiation) was placed in the bottom. Cells were allowed to migrate toward bottom for 6 hrs. Then cells were fixed and stained with DAPI. Representative images of migrated cells are shown and they were quantified using ImageJ software (n=3). B) Effect of irradiation on bone marrow derived macrophages (BMDM). Bone marrows were collected and induced to macrophages by CSF1 (10ng/ml) for 6 days. Cells were counted, seeded and subjected to 3Gy irradiation. Cells were collected 24hrs later, and RT-PCR was performed to detect RNA for the protumorigenic and inflammatory genes noted. C) BMDMs as prepared above were cultured in 50% tumor conditioned media + 50% complete DMEM for 24hrs. Cells were collected and assayed by RT-PCR for the genetic markers noted. D) Tumors collected as shown in Fig 1A were analyzed by FACS for MHCII expression on $CD11b^{+}F480^{+}$ macrophages. An increase in MHCII low-expressing macrophage population was observed. (* indicates significant changes with $P< 0.05$)

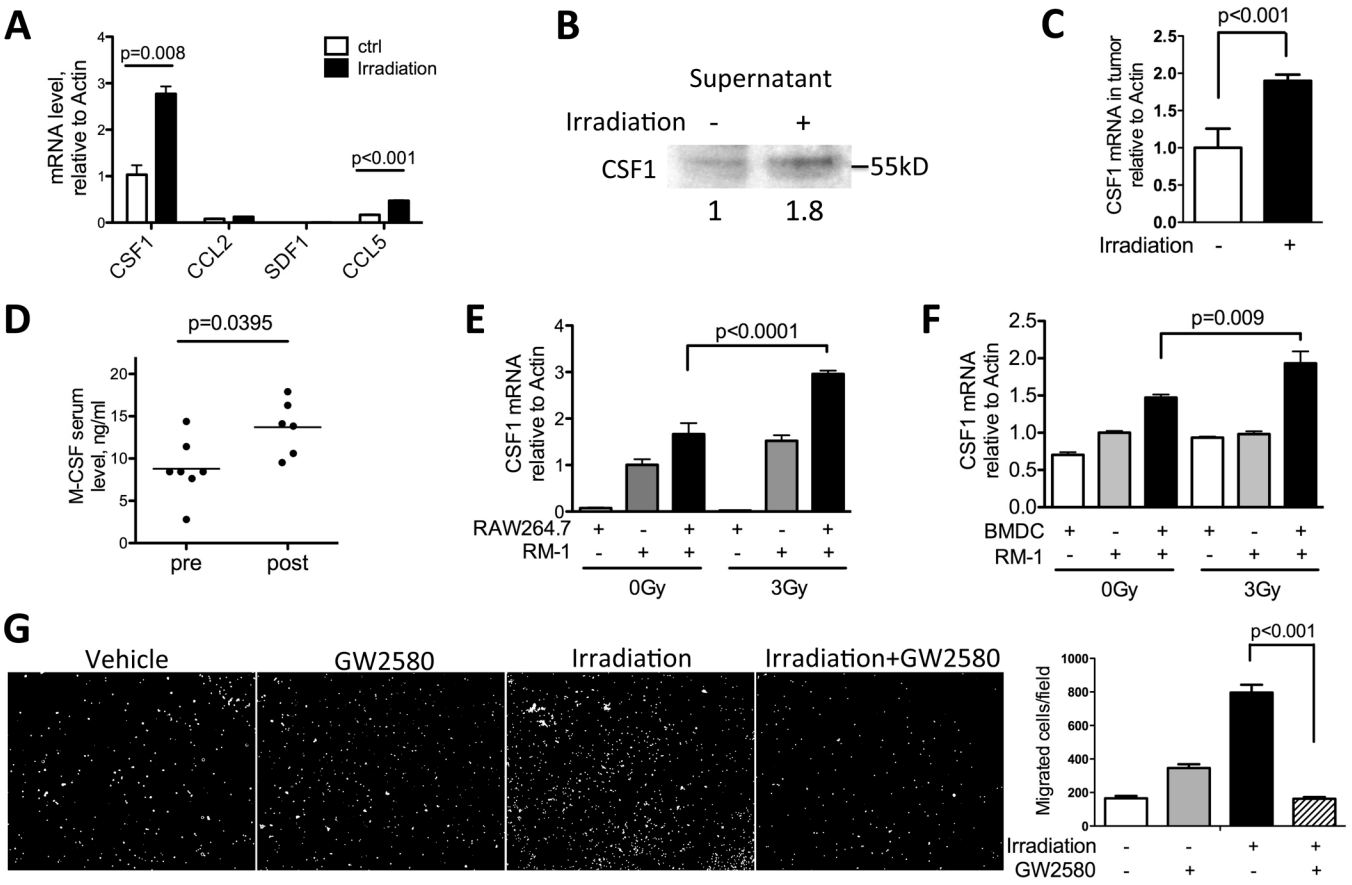

Figure 4. CSF1 expression is increased by irradiation

A) MycCaP cells were plated overnight and irradiated with 3Gy. Cells were collected 24 hrs after, and assayed by RT-PCR for factors known to recruit myeloid cells: CSF1, CCL2, SDF1 and CCL5. CSF1 is shown to have the highest expression and most significant increase. B) Conditioned media from Myc-CaP cells 48hrs after irradiation were collected, concentrated by centrifugation, normalized and analyzed by SDS-PAGE. Secreted CSF1 was detected at 50kDa. Relative expression level quantified by ImageJ was shown below the blot. C) Tumors collected as shown in Fig 1A were assayed by RT-PCR for CSF1 mRNA expression. D) Serum samples from prostate cancer patients pre- and post-radiotherapy were analyzed by ELISA for CSF1. E) RM-1 cells and macrophage cell line RAW264.7 were co-cultured overnight and irradiated with 3Gy. Cells were collected 24hrs and analyzed by RT-PCR for CSF1 mRNA. F) RM-1 cells and BMDM were co-cultured for 4hrs and irradiated with 3Gy. Cells were collected 24hrs and analyzed by RT-PCR for CSF1 mRNA. G) RAW264.7 macrophage migration assay was performed by using conditioned media in lower chamber, collected as in panel B. GW2580 (1μM) was added to the top chamber. Quantification of 9 fields was summarized in panel F. Representative images of migrated cells were shown in G.

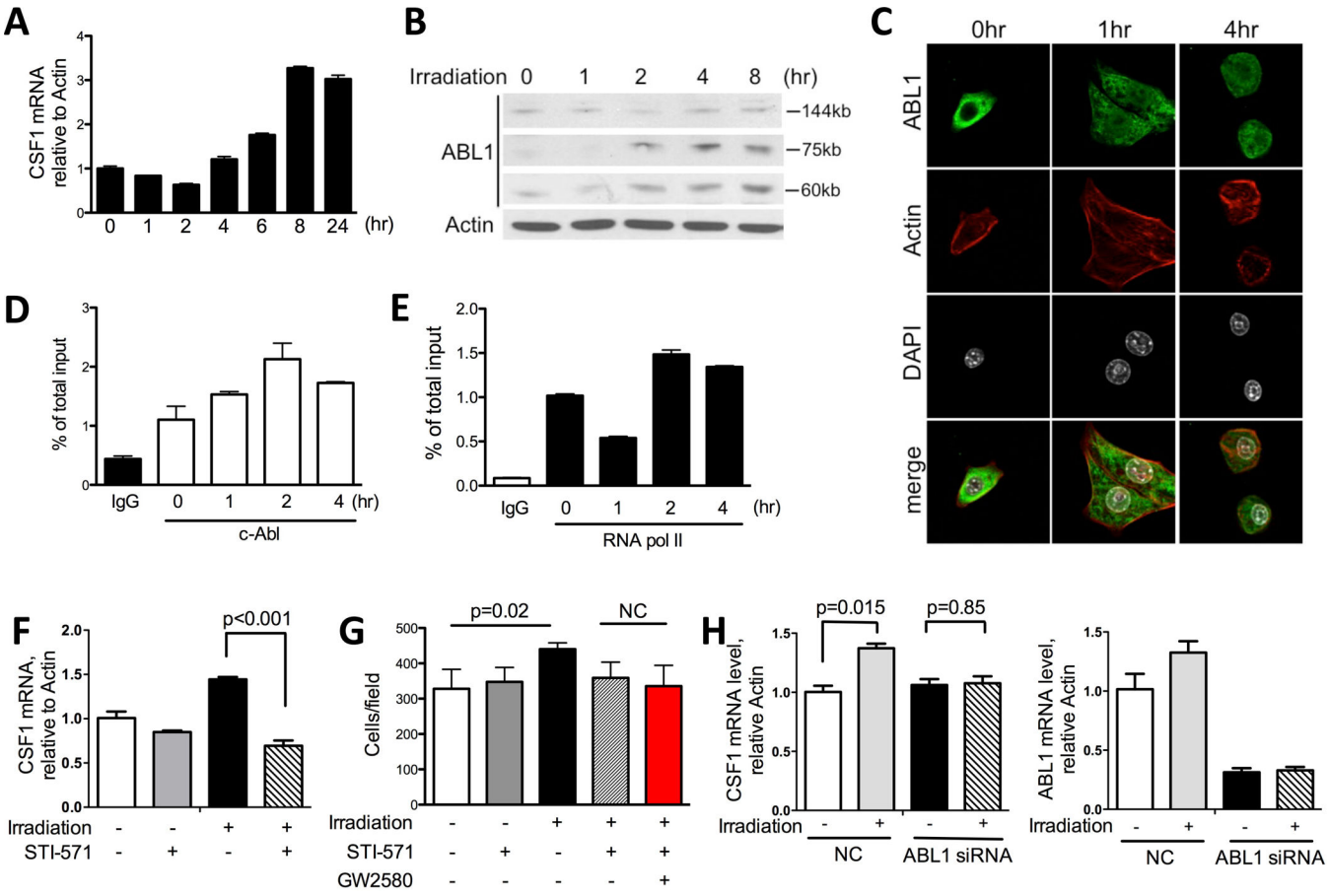

Figure 5. Irradiation induces CSF1 production through an ABL1-dependent mechanism

A) CSF1 mRNA expression in Myc-CaP cells 0, 1, 2, 4, 6, 8, and 24hrs after irradiation (3Gy). B) ABL1 is cleaved by irradiation *in vitro*. 4×10^5 Myc-CaP cells were plated in 6-well plate overnight and irradiated with 3Gy the next day. Cells were collected at 1, 2, 4, and 8 hrs after irradiation. Cells lysates were normalized and assayed by SDS-PAGE. Western blot was probed with ABL1 (K-12) antibody for both full length and cleaved ABL1. Two cleavage products, 60kD and 75kD, were detected. C) Confocal images of Myc-CaP cells at 1 and 4hrs after irradiation. Green: ABL1; red: actin; white: nucleus (DAPI). D–E) Myc-CaP cells 0, 1, 2, 4 hrs after irradiation were fixed in 3% PFA and processed for ChIP assay using c-Abl antibody (D) and RNA polymerase II antibody (E) as described in Material and Methods section. Rabbit IgG was used as negative control. F) Myc-CaP cells were irradiated with 3Gy and STI-571 (5μM) was added right after. Cells were collected 24hrs later and analyzed by RT-PCR for CSF1 mRNA expression. G) Migration assay using conditioned media collected as in panel F. GW2580 was added to the top chamber to examine the additive effects between STI-571 and GW2580. H) CSF1-mRNA in human prostate cancer cells after ABL1 directed RNAi. CWR22Rv1 cells were transfected with ABL1 siRNA and negative control (NC: non-specific siRNA). Cells were irradiated 30hrs after siRNA treatment and collected 24hrs after irradiation. Expression level of ABL1 was reduced to 30% of control after specific siRNA treatment (right panel). CSF1 mRNA was analyzed by RT-PCR with and without irradiation.

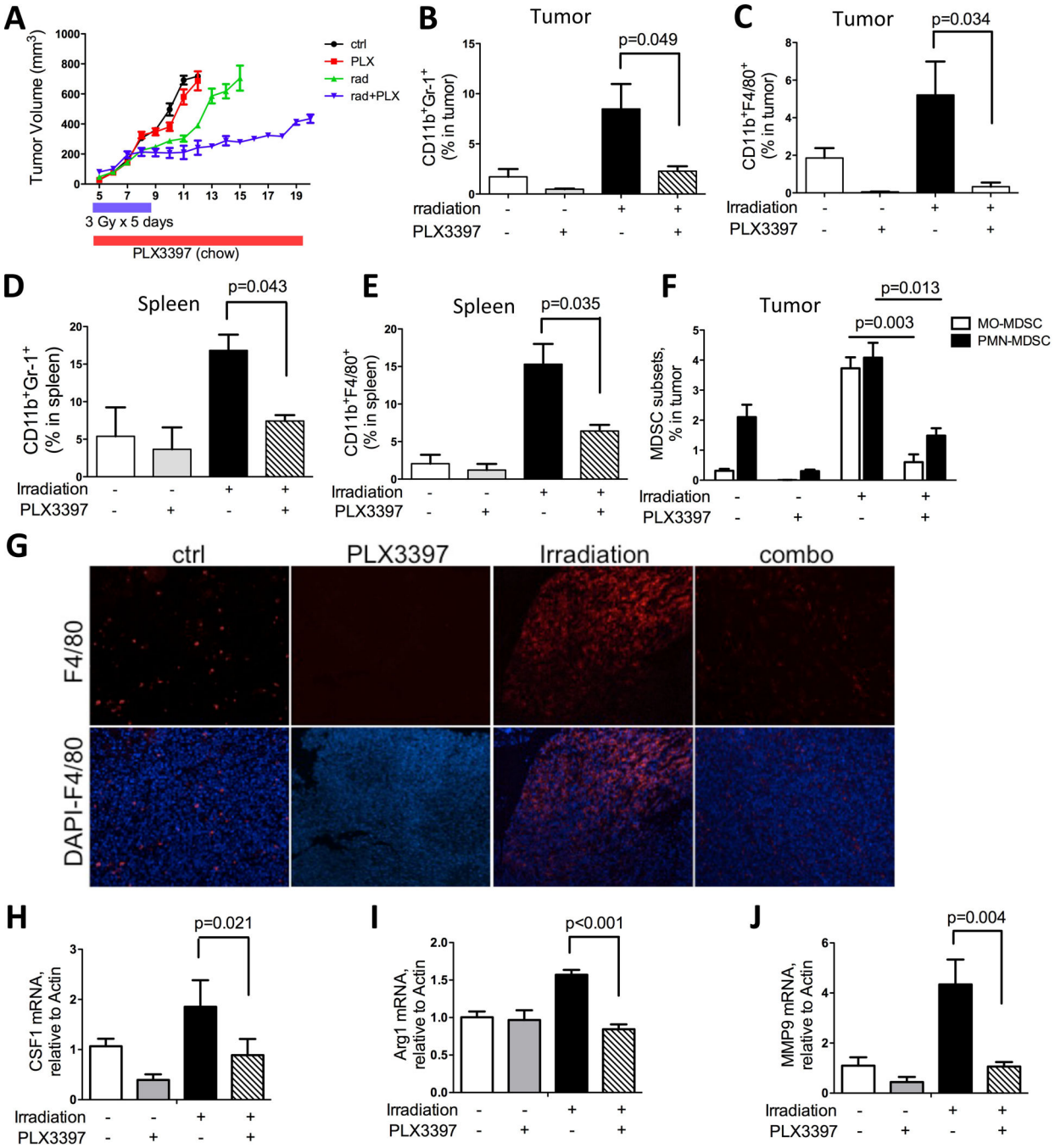

Figure 6. CSF1/CSF1R blockade inhibits tumor growth after irradiation

A) Growth curve of subcutaneous RM-1 tumors treated with RT (3Gy×5 days), PLX3397 (in food chow) or combination as indicated. Tumors were measured daily by caliper. B–C) FACS analysis of $CD11b^+F4/80^+$ macrophages and $CD11b^+Gr\text{-}1^+$ MDSCs in tumor, collected at end points (tumor n=6 × for each cohort). D–E) FACS analysis of $CD11b^+F4/80^+$ macrophages and $CD11b^+Gr\text{-}1^+$ MDSCs in spleen, at the same termination time as above. F) FACS analysis for MDSC subsets, MO-MDSC and PMN-MDSC with single or combination treatment. G) Representative immunohistochemsitry staining for

F4/80 on tumor sections with single or combination treatment. H–J) RT-PCR analysis of mRNA extracted from tumors for CSF1, MMP9 and Arg1.

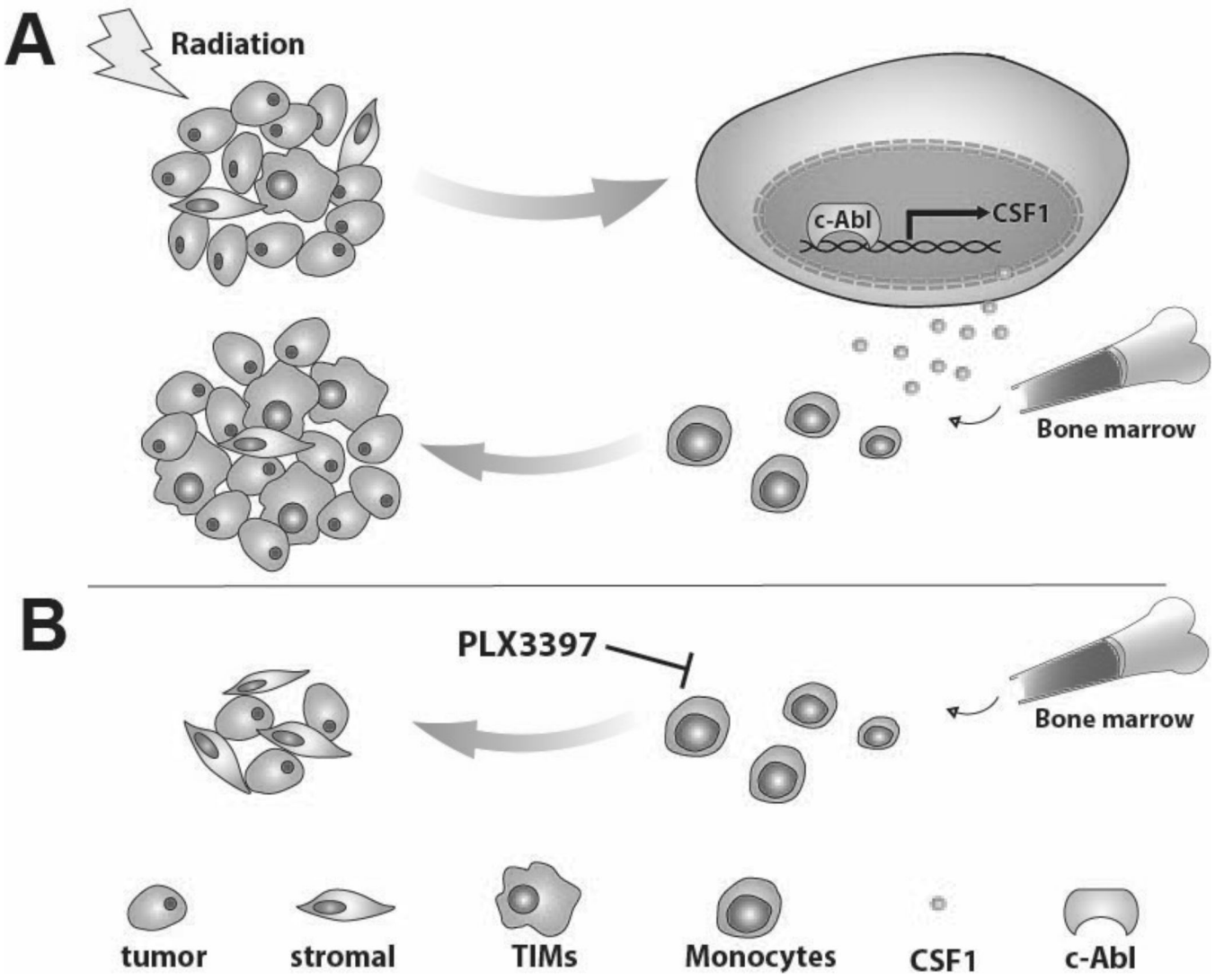

Figure 7. Model of CSF1 expression induced by irradiation, promoting TIMs recruitment and tumor regrowth

A) Tumor irradiation activates ABL1, which translocates to the nucleus, binding to the promoter region of CSF1 and up-regulates its gene expression. Additional TIMs are recruited to tumor sites due to the increase in CSF1 and they can thus promote tumor growth. B) When tumor-bearing mice were treated with a small molecule CSF1R kinase inhibitor, CSF1/CSF1R signaling is inhibited resulting in decreased infiltration of TIMs, reducing their tumor growth promoting influences.